A case of Langerhans cell sarcoma on the scalp: Whole‐exome sequencing reveals a role of ultraviolet in the pathogenesis

AUTHOR(S):

Katsuragawa, Hiroyuki; Yamada, Yosuke; Ishida, Yoshihiro; Kaku, Yo; Fujimoto, Masakazu; Kataoka, Tatsuki R.; Haga, Hironori

A Case of Langerhans Cell Sarcoma on the Scalp: Whole-Exome Sequencing Reveals a Role of Ultraviolet in the Pathogenesis

Hiroyuki Katsuragawa, MD[1], Yosuke Yamada, MD, PhD[1], Yoshihiro Ishida, MD, PhD[2], Yo Kaku, MD, PhD[2], Masakazu Fujimoto, MD, PhD[1], Tatsuki R. Kataoka, MD, PhD[1], and Hironori Haga, MD, PhD[1]

[1] Department of Diagnostic Pathology, Kyoto University Hospital, Kyoto, Japan

[2] Department of Dermatology, Kyoto University Hospital, Kyoto, Japan

Running head

UV Meets Langerhans Cell Sarcoma

Author Note

Corresponding author: Yosuke Yamada

Address: 54 Shogoin Kawahara-cho, Sakyo-ku, Kyoto 606-8507, Japan

Fax number: +81-75-751-3499

Phone number: +81-75-751-4946

Email: yyamada@kuhp.kyoto-u.ac.jp

There are no Abbreviated words in this submission

Abstract (200 words)

Langerhans cell sarcoma (LCS) is a high-grade neoplasm with overtly malignant cytological features and a Langerhans cell phenotype. The underlying genetic features are poorly understood, and only a few alterations, such as those of the MARK pathway-related genes, *CDKN2A* and *TP53* have been reported. Here we present a 70-year-old male with LCS on the scalp and pulmonary metastasis. The multinodular tumor, 3.0 cm in diameter, consisted of diffusely proliferated pleomorphic cells with numerous mitoses (53/10 HPFs). Immunohistochemically, the tumor cells were positive for CD1a, Langerin, and PD-L1, and the Ki-67 labeling index was 50%. These pathological features were consistent with LCS, and were also observed in the metastatic tumor. Whole-exome sequencing revealed that both the primary and metastatic tumors harbored a large number of mutations (>20 mutations/megabase), with deletion of *CDKN2A* and *TP53* mutation, and highlighted that the mutational signature was predominantly characteristic of ultraviolet (UV) exposure (W=0.828). Our results suggest, for the first time, that DNA damage by UV could accumulate in Langerhans cells and play a role in the pathogenesis of LCS. The high mutational burden and PD-L1 expression in the tumor would provide a rationale for the use of immune checkpoint inhibitors for treatment of unresectable LCS.

Keywords: CDKN2A, Langerhans Cell Histiocytosis, Langerhans Cell Sarcoma, MAPK pathway, PD-L1, Whole Exome Sequencing, TP53, Ultraviolet

Introduction

Langerhans cell sarcoma (LCS) is an aggressive neoplasm with apparent malignant cytological features and a Langerhans cell phenotype. It is extremely rare, with an incidence of 0.2 per 10,000,000 population (1), and often develops in skin and underlying soft tissues, mostly in adults. Microscopically, LCS consists of atypical pleomorphic cells, sometimes with the complex grooves reminiscent of Langerhans cells. The tumor shows high proliferative activity, and mitotic figures often exceed >50/10 high-power fields. Demonstration of a Langerhans cell phenotype by immunohistochemistry or by examination of the ultrastructure is required for diagnosis. The prognosis is poor, with a median overall survival period of only 19 months (1, 2).

These clinical and pathological features are considerably different from those of Langerhans cell histiocytosis (LCH), the most common form of Langerhans cell neoplasm. LCH often develops in children, especially as a bone tumor. It does not show obvious cytological atypia, although the phenotypic features resemble LCS, and it generally exhibits indolent behavior, sometimes even showing spontaneous regression (2).

However, the underlying molecular features of LCS that could explain its aggressive behavior or pathogenesis, and lead to the development of more effective treatment strategies, are poorly understood, except for the reported presence of a few genetic alterations, such as mutations of MAPK-related genes, *CDKN2A*, or *TP53* (3-8).

Here, we report a case of LCS on the scalp of an elderly male with pulmonary metastasis. As well as histological and immunohistochemical analyses, we performed whole-exome sequencing for both the primary and metastatic sites and attempted to clarify the molecular features.

Clinical summary

The patient was a 70-year-old male who had been treated for prostate cancer ten years previously. He had no history of any hematopoietic malignancy. Three months before presentation, he had undergone surgery for cervical spondylotic myelopathy. During the postoperative rehabilitation period, a 3.0-cm nodule was found on the scalp, corresponding to a site the patient reported to have been struck hard against a showerhead two years previously. A biopsy and histologic examination of the scalp tumor suggested LCS. Computed tomography (CT) for systemic screening revealed a nodule 1.0 cm in diameter in the upper lobe of the left lung. This was suspected to be a metastasis of the LCS, as it had not been detected in a CT examination performed six months previously. 18F-fluorodeoxyglucose (18F-FDG) positron emission tomography (FDG-PET) demonstrated no other possible metastatic tumors other than that in the lung. The patient underwent resection of the scalp tumor and received two courses of CHOP (cyclophosphamide, hydroxydaunorubicin, oncovin, and prednisone) therapy. However, as the lung nodule gradually enlarged, it was resected for pathological examination.

Pathological findings

Macroscopically, the scalp tumor formed an irregular nodule 3.0 cm in diameter. The formalin-fixed specimen showed that a whitish-gray tumor had invaded the periosteum from the epidermis (Figure S1A-B). Microscopically, the tumor consisted of a diffuse proliferation of atypical cells, which had pleomorphic nuclei with complex grooves, conspicuous nucleoli, and moderate amounts of cytoplasm (Figure 1A-B). Mitotic figures were plentiful (53/10 HPFs), and variable numbers of eosinophils and small lymphocytes were present within the tumor (Figure 1C-D). Immunohistochemistry (IHC) showed that the tumor cells were

positive for CD1a, CD4, CD68, Langerin, and S-100. The Ki-67 labeling index was about 50% (Figure 1E-H). BRAF V600E, CD21, CD23, CD123, CD163, MCPyV, and SOX10 were negative (data not shown). These pathological features were consistent with Langerhans cell sarcoma (LCS). There were no areas containing proliferations of bland histiocytic cells, which is a feature reminiscent of Langerhans cell histiocytosis (LCH). The resected lung tumor also consisted of atypical cells with a morphology and immunophenotype similar to the skin tumor, although they are more pleomorphic than tumor cells in the primary site (Figure 2A-D). Thus, this was diagnosed as a metastasis from the LCS on the scalp.

We next performed whole-exome sequencing (WES) for both the primary and metastatic tumors to clarify the genetic profile. Both tumors harbored a large number of mutations (663 SNVs/indels in the primary site and 634 SNVs/indels in the metastasis), most of which (569 genes) were shared between the two lesions (Figure 3A), including *TP53*/Y88C, *KMT2D*/R3703X, and *STK19*/G265A mutations (Table 1). Copy number analysis showed that both tumors harbored homozygous deletions in 6q and 9p, the latter being consistent with the locus of *CDKN2A* (Figure 3B and Figure S2A-B). The *TP53* mutation and *CDKN2A* deletion were supported by the findings of IHC because the tumor cells were strongly positive for p53 and negative for p16, the protein encoded by *CDKN2A* (Figure 4A-B). Because the number of mutations was large, we were able to decompose the mutational signature into known COSMIC signatures; surprisingly, it was dominated by COSMIC signature 7, i.e., an ultraviolet (UV)-mutational signature (W=0.828) (Figure 3C and Figure S2C). The mutation spectra further supported the role of UV in the mutagenesis: 77.3% (primary site) and 77.1% (metastatic site) of the SNVs were C to T mutations at dipyrimidine sites, and 5.4% (primary) and 4.5% (metastatic) of them were CC to TT substitutions (9).

Considering its possible therapeutic relevance, we also performed immunohistochemistry for PD-L1 and confirmed that both the primary and metastatic tumors partially expressed PD-L1, as well as accompanying macrophages (Figure 4C).

Discussion

A literature searched revealed ten English-language papers reporting genetic alterations in LCS (3-8, 10-13). Six case reports (3-8), three of which included WES data (4-6), indicated causative alterations such as mutations related to activation of the MAPK pathway (*BRAF*, *KRAS*, *MAPK2A1*, or *NRAS*), homozygous deletions of *CDKN2A/(2B)*, and/or a loss-of-function mutation of *TP53* (Table 1). The present case also exhibited *CDKN2A* deletion and a pathogenic missense mutation in *TP53* (Figure 3B and Table 1), which was supported by IHC (Figure 4A-B). Xerri et al. reported that deletion of *CDKN2A/(2B)* was not found among their 22 LCS samples (3), and Badalian detected *TP53* mutation in only one of 61 LCH cases (14), while mutations related to the MAPK pathway overlapped in LCS and LCH (14, 15). Thus, the dysfunction of these common tumor suppressor genes would underlie the aggressiveness of LCS and differentiate it from LCH. The present case also harbored truncating mutations of *KMT2D* and *STK19*, which are also known to be tumor suppressor genes in some cancers including those of the skin (16).

Our most important discovery in the present case was that the mutational signature was highly correlated with that of UV mutagenesis (Figure 3C). Murine experiments have shown that Langerhans cells have a rather long lifespan (at least 18 months) (17), and UV can change the phenotype of human Langerhans cells through alteration of the surface molecules (18). Through our analysis of this Langerhans cell neoplasm, we demonstrated for the first time that UV could affect not only the phenotype but also the genome of the Langerhans cells.

LCS can arise through at least three mechanisms: *de novo*, progression from LCH, and transdifferentiation from a B-cell neoplasm (4, 10, 12, 19). Our results suggest that *de novo* LCS, corresponding to our case, can occur as a UV-related cancer, as is the case for skin cancers of various lineages (e.g., basal cell carcinoma, squamous cell carcinoma, and melanoma, etc.). The association of UV with LCS could also explain the tendency of LCS to arise more frequently in adult skin, including sun-exposed areas, in comparison with LCH. Taken together, we speculate that if human Langerhans cells are able to remain in the epidermis for a sufficient period of time as murine Langerhans cells (17), ultraviolet (i.e., sun) exposure could cause genetic alterations (some of the genes might be related to their migration capacity), ultimately leading to their malignant transformation (i.e., [*de novo*] LCS) (Figure 4D).

Unfortunately, we were unable to detect any possible driver mutations. As well as the typical histological features, because IHC showed the tumor to be strongly positive for EZH2 (Figure S1C), whose expression is known to be highly correlated with the phosphorylation of ERK in histiocytic and dendritic cell neoplasms (20), we speculate that the present case might also have been driven by the MAPK pathway through unknown mechanisms. However, other pathways may play a key role in the pathogenesis, as has been reported for some LCH cases (15).

Lastly, we attempted to consider some therapeutic options for LCS, as few established treatments are currently available. Because the tumor showed a high tumor mutation burden (>20/Mb), we speculated that immune checkpoint inhibitors might be an option, especially as the tumor cells expressed PD-L1 (Figure 4C). Although no previous reports have documented the use of this type of drug for Langerhans cell neoplasms, in view of the generally dismal

prognosis of LCS, our present findings suggest that immune checkpoint inhibitors would be worth considering for unresectable cases, under careful monitoring.

In summary, we have reported a patient with LCS on the scalp associated with pulmonary metastasis. As well as the typical pathological features, exome sequencing revealed that the tumor harbored a large number of mutations, including *CDKN1A* deletion and *TP53* mutation, and strongly suggested that the mutations had arisen through UV exposure. These findings advance our understanding of the biology of Langerhans cells and their neoplasms, and might contribute to the development of more effective treatment strategies.

Disclosure Statement

The authors have no conflicts of interest to declare.

Author Contributions

Drafting the manuscript and figures; HK and YY. Acquisition and analysis of data; YI. Correction and approval of manuscript; All authors.

Figure Legends

Figure 1. Microscopic features of the primary tumor (skin) (A-D, H&E sections; E-H, immunohistochemistry).

A multinodular tumor is evident on the scalp (A). The tumor cells have pleomorphic nuclei with complex grooves, conspicuous nucleoli, and moderate amounts of cytoplasm (B), with numerous mitoses (arrows) (C). Focal eosinophilic infiltration is evident (D). The tumor cells are positive for CD1a (E), Langerin (F) and S-100 (G), and the Ki-67 labeling index was 50% (H).

Figure 2. Microscopic features of the metastatic tumor (lung) (A-B, H&E sections; C-D, immunohistochemistry).

A nodule 10 mm in diameter is evident in the lung (A). The tumor consists of highly atypical cells morphologically similar to those at the primary site, with necrosis (upper right) (B). The tumor cells are positive for CD1a (C) and Langerin (D).

Figure 3. Whole-exome sequencing of the primary and metastatic tumors.

Variant allele frequency (VAF) in the primary and metastatic tumors (A). Both tumors harbor a large number of genomic mutations, which are mostly shared between the two lesions, including mutations in *TP53*, *KMT2D*, and *STK11* (A). Copy number analysis of the primary tumor (B-C). The tumor exhibits a homozygous deletion of 9q (B), which corresponds to the locus of *CDKN2A* (C). The mutational signature of the tumor is highly correlated with COSMIC signature 7, i.e., an ultraviolet mutational signature (D).

Figure 4. Immunohistochemistry for p16, p53, and PD-L1 in the primary tumor, and a possible role of ultraviolet in the pathogenesis of Langerhans cell sarcoma: a hypothesis.

The tumor is completely negative for p16 (A) and strongly/diffusely positive for p53 (B). Some of the tumor cells, including one with mitosis (arrow), exhibit membranous PD-L1 expression (C). A possible role of ultraviolet in the pathogenesis of Langerhans cell sarcoma: a hypothesis (D). If human Langerhans cells remain in the epidermis for a sufficient period of time, ultraviolet (i.e., sun) exposure could cause genetic alterations, ultimately leading to their malignant transformation (i.e., [*de novo*] LCS).

Table

Table 1. Reported genetic alterations in Langerhans cell sarcoma.

Supplementary information

Figure S1. Macroscopic and immunohistochemical features of the skin tumor.

The multinodular whitish tumor with a diameter of 3.0 cm is seen on the skin (A). The cut section of the tumor shows expansion from the epidermis to the periosteum (B). The tumor is diffusely positive for EZH2 (C).

Figure S2. Whole-exome sequencing of the primary and metastatic tumors.

The primary tumor shows a homozygous deletion of 6p (A). The copy number validation of the metastatic tumor is common to that of the primary tumor (B). The

220 mutational signature of the metastatic tumor is highly correlated with COSMIC signature 7,

221 i.e., an ultraviolet mutational signature (C).

References

1. Tella SH, Kommalapati A, Rech KL, Go RS, Goyal G. Incidence, Clinical Features, and Outcomes of Langerhans Cell Sarcoma in the United States. *Clin Lymphoma Myeloma Leuk*. 2019;**19**:441-6.
2. Swerdlow SH, Campo E, Harris NL, et al. *WHO Classification of Tumours of Haematopoietic and Lymphoid Tissues*. Lyon: IARC; 2017.
3. Xerri L, Adélaïde J, Popovici C, et al. CDKN2A/B Deletion and Double-hit Mutations of the MAPK Pathway Underlie the Aggressive Behavior of Langerhans Cell Tumors. *Am J Surg Pathol*. 2018;**42**:150-9.
4. Choi SM, Andea AA, Wang M, et al. KRAS mutation in secondary malignant histiocytosis arising from low grade follicular lymphoma. *Diagn Pathol*. 2018;**13**:78.
5. Kim SW, Choi MK, Han HS, et al. A Case of Pulmonary Langerhans Cell Sarcoma Simultaneously Diagnosed with Cutaneous Langerhans Cell Histiocytosis Studied by Whole-Exome Sequencing. *Acta Haematol*. 2017;**138**:24-30.
6. Karai LJ, Sanik E, Ricotti CA, Susa J, Sinkre P, Aleodor AA. Langerhans cell sarcoma with lineage infidelity/plasticity: a diagnostic challenge and insight into the pathobiology of the disease. *Am J Dermatopathol*. 2015;**37**:854-61.
7. Mourah S, Lorillon G, Meignin V, et al. Dramatic transient improvement of metastatic BRAF(V600E)-mutated Langerhans cell sarcoma under treatment with dabrafenib. *Blood*. 2015;**126**:2649-52.
8. Zwerdling T, Won E, Shane L, Javahara R, Jaffe R. Langerhans cell sarcoma: case report and review of world literature. *J Pediatr Hematol Oncol*. 2014;**36**:419-25.
9. Alexandrov LB, Nik-Zainal S, Wedge DC, et al. Signatures of mutational processes in human cancer. *Nature*. 2013;**500**:415-21.
10. Ambrosio MR, De Falco G, Rocca BJ, et al. Langerhans cell sarcoma following marginal zone lymphoma: expanding the knowledge on mature B cell plasticity. *Virchows Arch*. 2015;**467**:471-80.
11. Chang NY, Wang J, Wen MC, Lee FY. Langerhans Cell Sarcoma in a Chronic Myelogenous Leukemia Patient Undergoing Imatinib Mesylate Therapy: A Case Study and Review of the Literature. *Int J Surg Pathol*. 2014;**22**:456-63.
12. Muslimani A, Chisti MM, Blenc AM, Boxwala I, Micale MA, Jaiyesimi I. Langerhans/dendritic cell sarcoma arising from hairy cell leukemia: a rare phenomenon. *Ann Hematol*. 2012;**91**:1485-7.
13. Shao H, Xi L, Raffeld M, et al. Clonally related histiocytic/dendritic cell sarcoma and chronic lymphocytic leukemia/small lymphocytic lymphoma: a study of seven cases. *Mod Pathol*. 2011;**24**:1421-32.

14. Badalian-Very G, Vergilio JA, Degar BA, et al. Recurrent BRAF mutations in Langerhans cell histiocytosis. *Blood*. 2010;**116**:1919-23.
15. Diamond EL, Durham BH, Haroche J, et al. Diverse and Targetable Kinase Alterations Drive Histiocytic Neoplasms. *Cancer Discov*. 2016;**6**:154-65.
16. Hodis E, Watson IR, Kryukov GV, et al. A landscape of driver mutations in melanoma. *Cell*. 2012;**150**:251-63.
17. Merad M, Manz MG, Karsunky H, et al. Langerhans cells renew in the skin throughout life under steady-state conditions. *Nat Immunol*. 2002;**3**:1135-41.
18. Aberer W, Schuler G, Stingl G, Hönigsmann H, Wolff K. Ultraviolet light depletes surface markers of Langerhans cells. *J Invest Dermatol*. 1981;**76**:202-10.
19. Nakamine H, Yamakawa M, Yoshino T, Fukumoto T, Enomoto Y, Matsumura I. Langerhans Cell Histiocytosis and Langerhans Cell Sarcoma: Current Understanding and Differential Diagnosis. *J Clin Exp Hematop*. 2016;**56**:109-18.
20. Tian X, Xu J, Fletcher C, Hornick JL, Dorfman DM. Expression of enhancer of zeste homolog 2 (EZH2) protein in histiocytic and dendritic cell neoplasms with evidence for p-ERK1/2-related, but not MYC- or p-STAT3-related cell signaling. *Mod Pathol*. 2018;**31**:553-61.

Figure 1

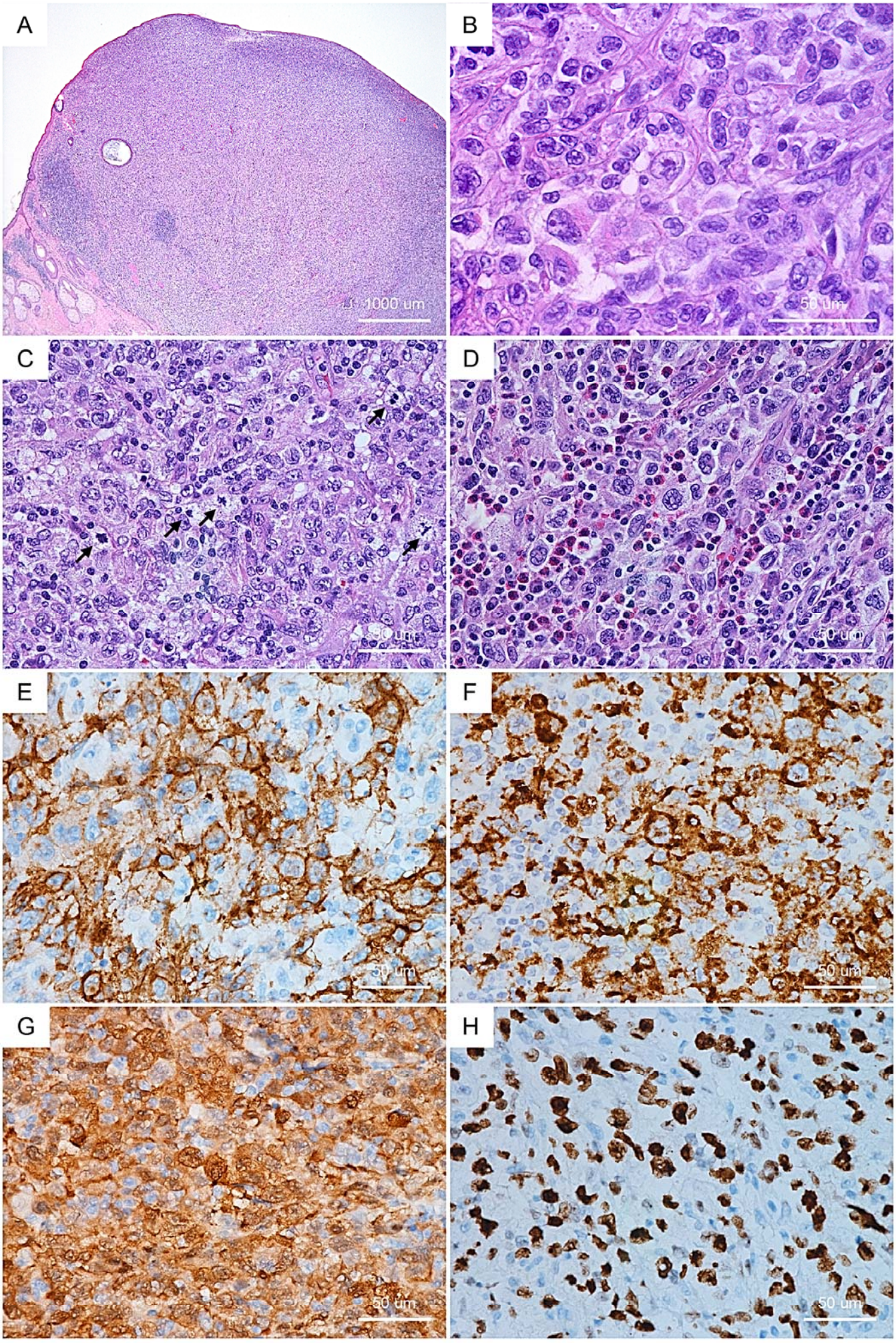

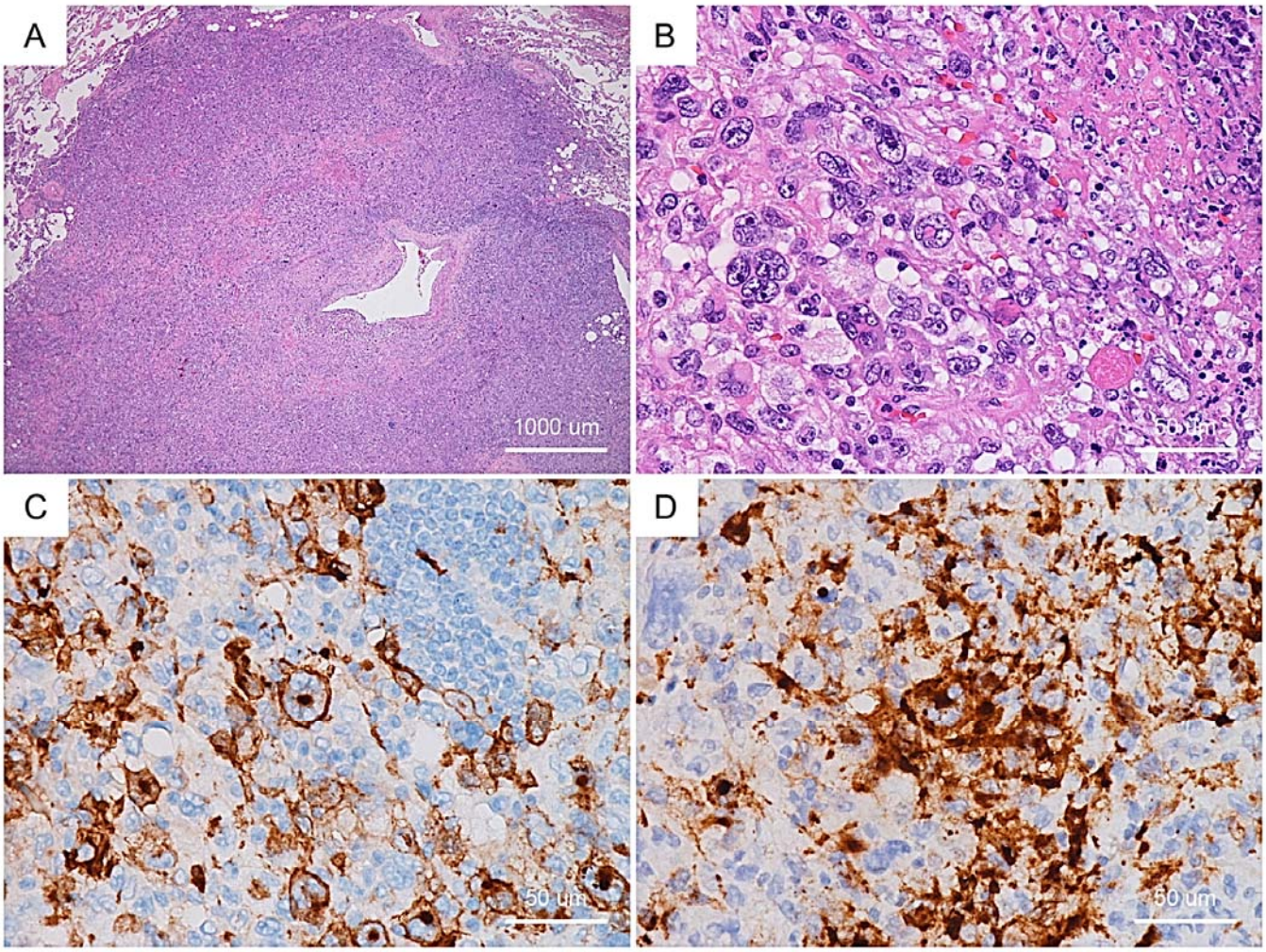

Figure 3

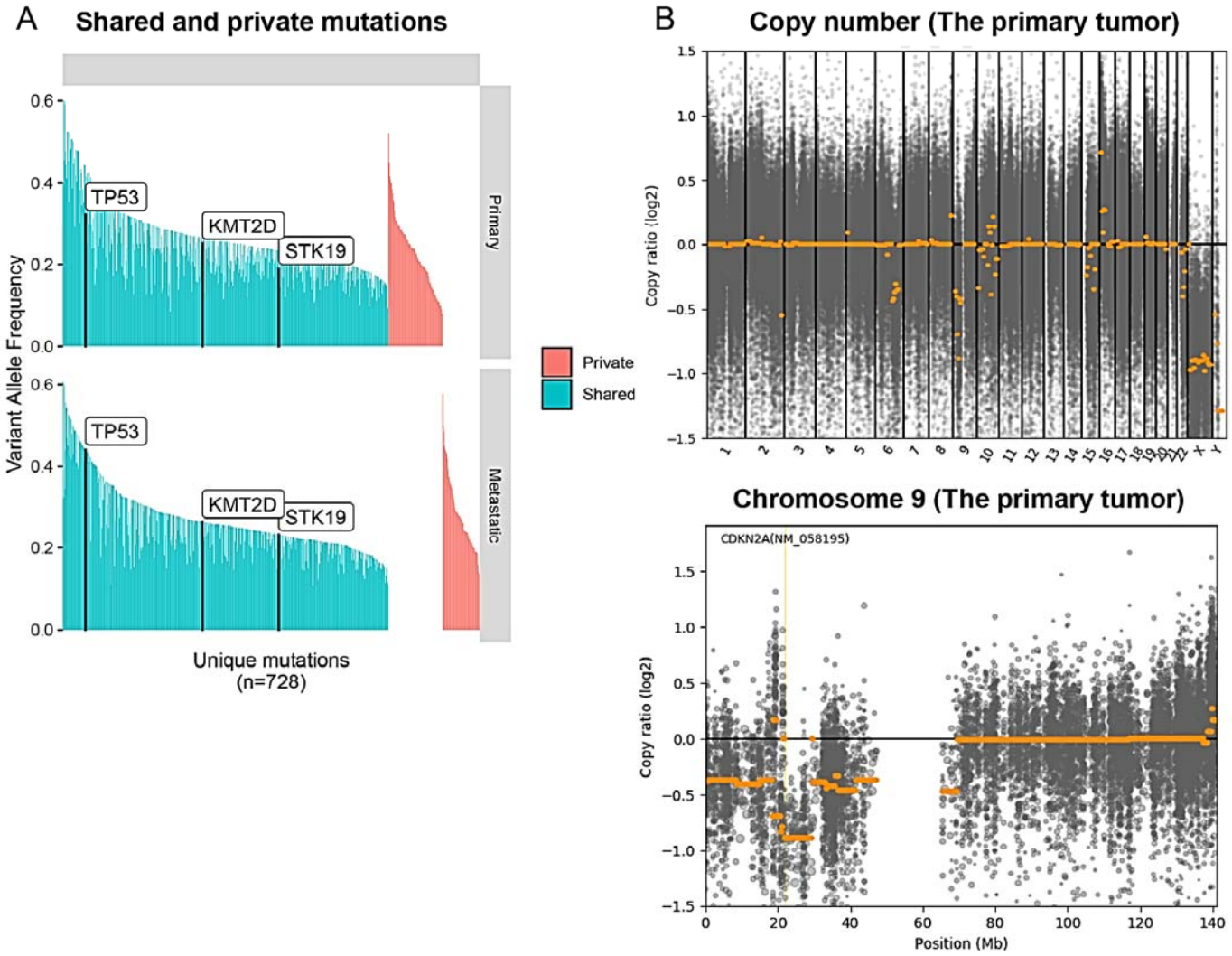

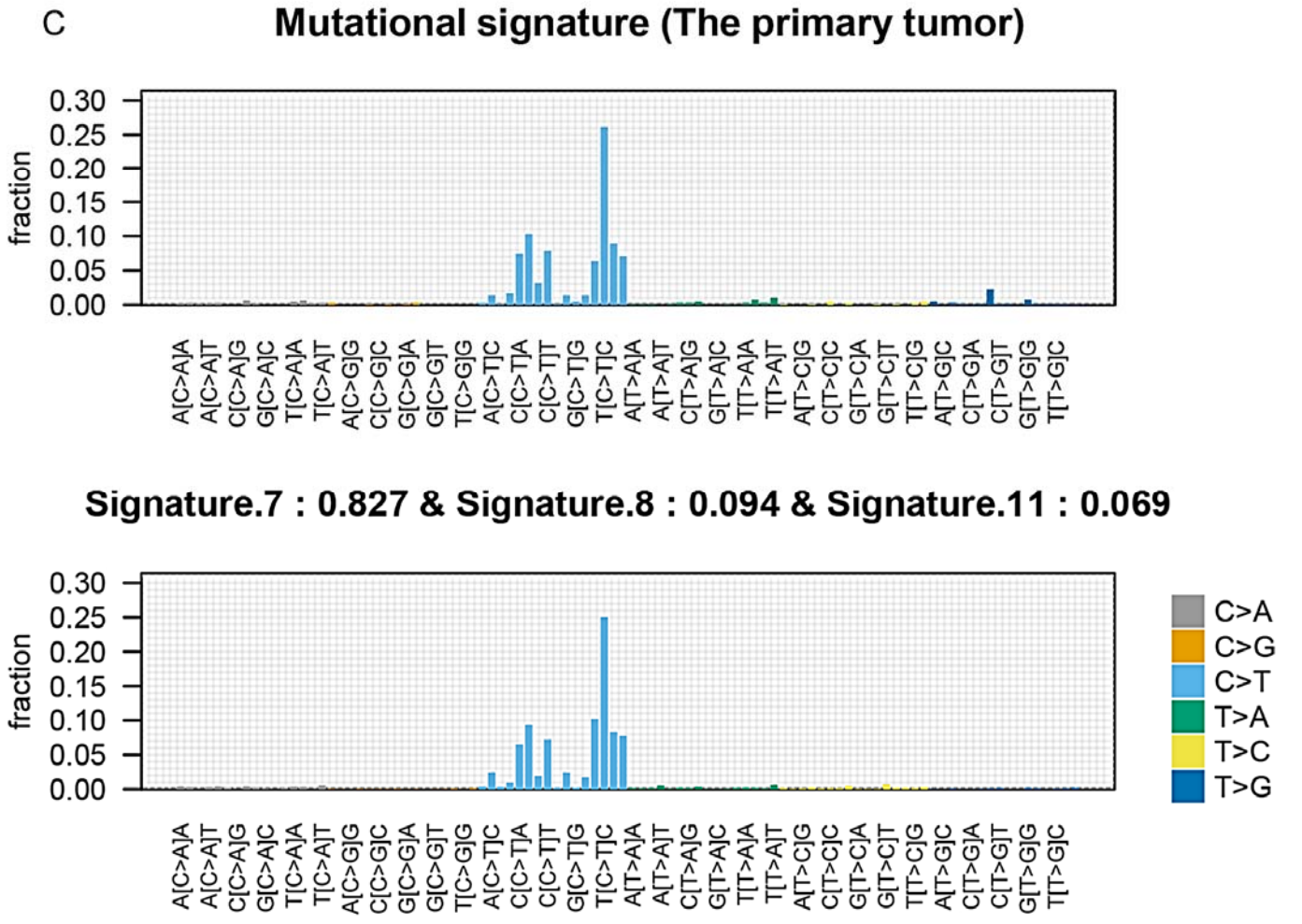

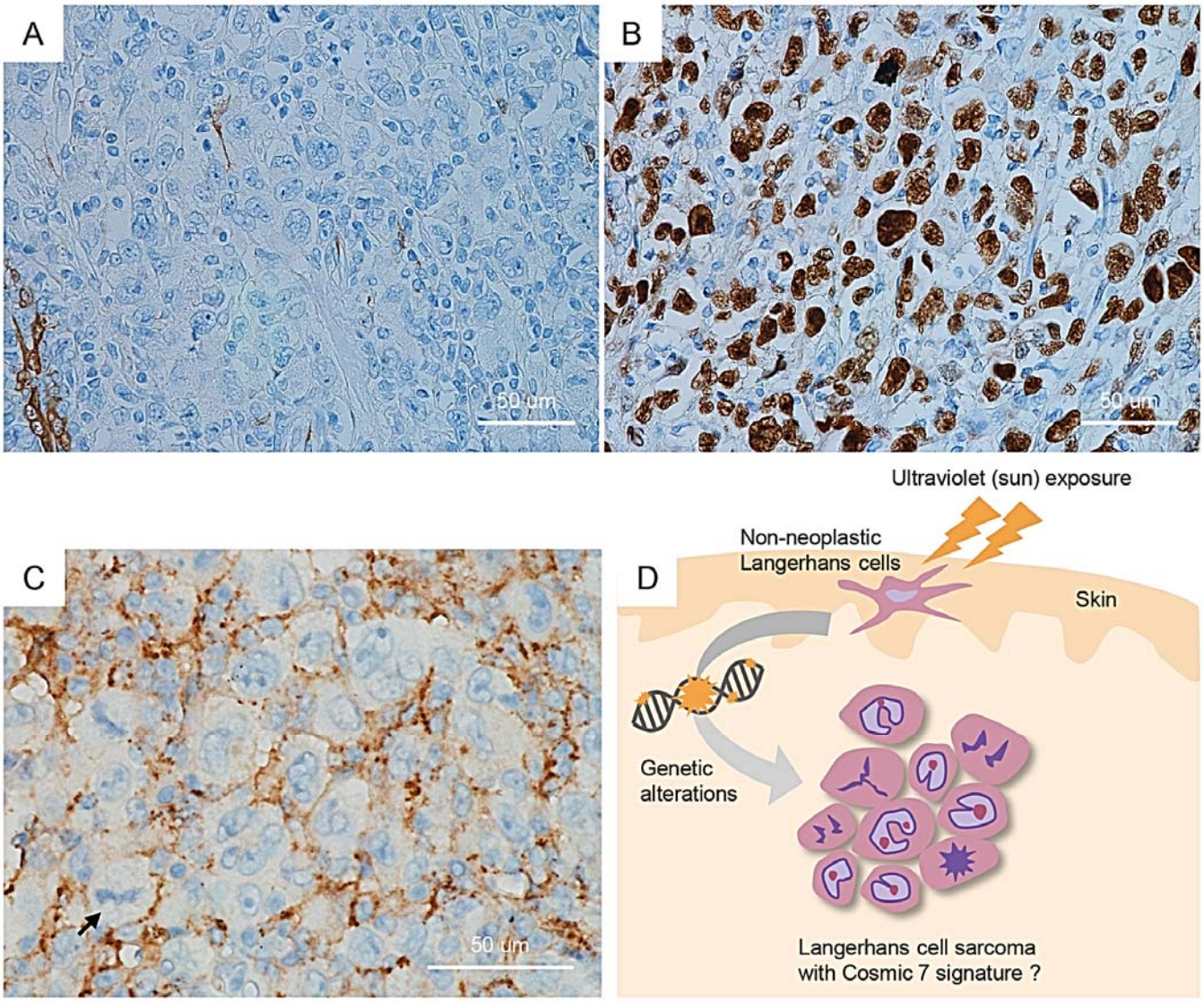

Table 1. Reported genetic alterations in Langerhans cell sarcoma

Authors	Age	Gender	Organ	Pathogenic genetic alterations	The primary tumor
The present case	70	Male	Skin	*KMT2D* (R3703X)	*De novo*
				STK19 (G265A)	
				TP53 (Y88C)	
Choi et al., 2018 (4)	NA	NA	Lymph node	*IgH/BCL2* (rearrangement)	Follicular lymphoma
				KRAS (G13D)	
Xerri et al., 2018 (3)	55	Male	Lymph node	*CDKN2A/B* (homozygous deletion)	*De novo*
				KMT2D (E2989X)	
				MAP2K1 (C121S)	
				NOTCH1 (Q2403X)	
				NRAS (Q61K)	
Kim et al., 2017 (5)	73	Male	Lung	*TP53* (R196*)	*De novo*
Karai et al., 2015 (6)	62	Female	Skin	*CDKN2A* (homozygous deletion)	*De novo*
				KRAS (Q61H)	
				TP53 (R282W)	
Mourah et al., 2015 (7)	58	Male	Lymph node	*BRAF* (V600E)	*De novo*
Zwerdling et al., 2014 (8)	7	Female	Soft tissue	*BRAF* (V600E)	*De novo*

NA, not available

Figure S1

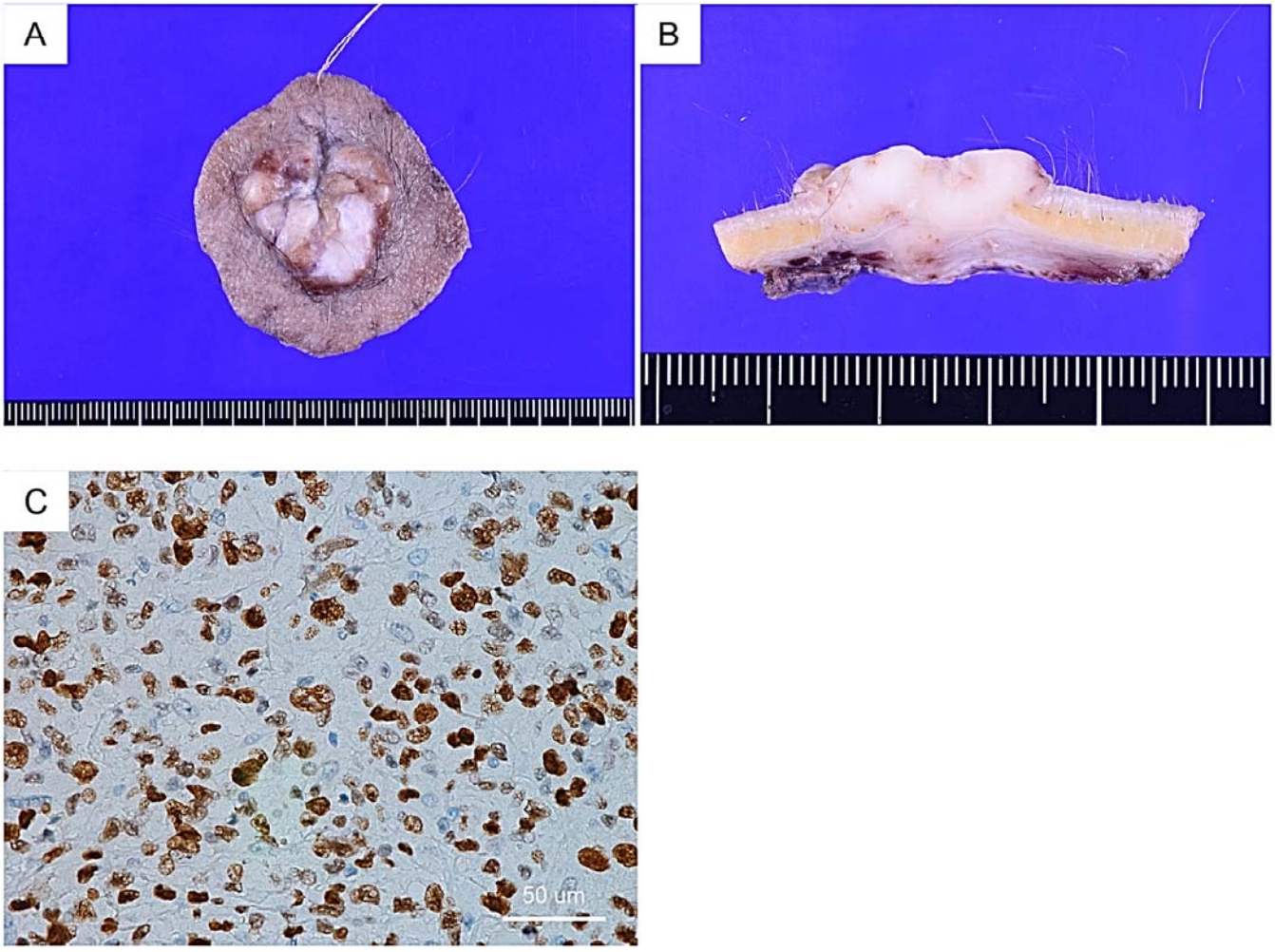

Figure S2